ECCM21

02-05 July 2024 | **Nantes - France**

Proceedings of the 21st European Conference on Composite Materials

Vol 8

Special Sessions

WWW.ECCM21.ORG

UNDER THE PATRONAGE OF:

ESCM European Society For Composite Materials

AMAC Association pour les MAtériaux Composites

EuCIA The European Voice of Composites

WITH THE SUPPORT OF:

RÉGION PAYS DE LA LOIRE

ORGANIZED BY:

CENTRALE NANTES

Nantes Université

SUPPORTING PARTNER:

JEC CONNECTING THE WORLD WITH COMPOSITES

Edited by:

Prof. Christophe BINETRUY
ECCM21 Conference Chair
Institute of Civil Engineering and Mechanics (GeM)
Centrale Nantes
Nantes Université

Prof. Frédéric JACQUEMIN
ECCM21 Conference Co-Chair
Institute of Civil Engineering and Mechanics (GeM)
Nantes Université

Published by:

The European Society for Composite Materials (ESCM) and the Ecole Centrale de Nantes.

©2024 ECCM21/The publishers
The Proceedings are published under the CC BY-NC 4.0 license in electronic format only, by the Publisher. The CC BY-NC 4.0 license permits non-commercial reuse, transformation, distribution, and reproduction in any medium, provided the original work is properly cited. For commercial reuse, please contact the authors. For further details please read the full legal code at:
http://creativecommons.org/licenses/by-nc/4.0/legalcode

These Proceedings have an ISBN (owned by the Publisher) and a DOI (owned by the Ecole Centrale de Nantes).

ISBN: 978-2-912985-01-9
DOI: 10.60691/yj56-np80

The Authors retain every other right, including the right to publish or republish the article, in all forms and media, to reuse all or part of the article in future works of their own, such as lectures, press releases, reviews, and books for both commercial and non-commercial purposes.*

Disclaimer:

The ECCM21 organizing committee and the Editors of these proceedings assume no responsibility or liability for the content, statements and opinions expressed by the authors in their corresponding publication.

CONTENTS

Editorial

Each volume gathers contributions on specific topics:

Vol 1. Industrial applications
Vol 2. Material science
Vol 3. Material and Structural Behavior – Simulation & Testing
Vol 4. Experimental techniques
Vol 5. Manufacturing
Vol 6. Multifunctional and smart composites
Vol 7. Life cycle performance
Vol 8. Special Sessions

This collection contains the proceedings of the 21st European Conference on Composite Materials (ECCM21), held in Nantes, France, July 2-5, 2024. ECCM21 is the 21st in a series of conferences organized every two years by the members of the European Society of Composite Materials (ESCM). As some of the papers in this collection show, this conference reaches far beyond the borders of Europe.

The ECCM21 conference was organized by the Nantes Université and the Ecole Centrale de Nantes, with the support of the Research Institute in Civil and Mechanical Engineering (GeM).

Nantes, the birthplace of the novelist Jules Verne, is at the heart of this edition, as are the imagination and vision that accompany the development of composite materials. They are embodied in the work of numerous participants from the academic world, but also of the many industrialists who are making a major contribution to the development of composite materials. Industry is well represented, reflecting the strong presence of composites in many application areas.

With a total of 1,064 oral and poster presentations and over 1,300 participants, the 4-day event enabled fruitful exchanges on all aspects of composites. The topics that traditionally attracted the most contributions were fracture and damage, multiscale modeling, durability, aging, process modeling and simulation and additive manufacturing.

However, the issues of energy and environmental transition, and more generally the sustainability of composite solutions, logically appear in this issue as important contextual elements guiding the work being carried out. This includes bio-sourced composites, material recycling and reuse of parts, the environmental impact of solutions, etc.

We appreciated the high level of research presented at the conference and the quality of the submissions, some of which are included in this collection. We hope that all those interested in the progress of European composites research in 2024 will find in this publication sources of inspiration and answers to their questions.

Prof. Christophe BINETRUY
ECCM21 Conference Chair
Institute of Civil Engineering and Mechanics (GeM)
Centrale Nantes
Nantes Université

Prof. Frédéric JACQUEMIN
ECCM21 Conference Co-Chair
Institute of Civil Engineering and Mechanics (GeM)
Nantes Université

CONTENTS

Under the Patronage of:

ESCM European Society For Composite Materials

AMAC Association pour les MAtériaux Composites

EuCIA The European Voice of Composites

Organized by: CENTRALE NANTES — Nantes Université

With the support of: RÉGION PAYS DE LA LOIRE

Supported by: EMC2 — JEC CONNECTING THE WORLD WITH COMPOSITES

Sponsored by:

Bronze Partner: BRUKER — INSTRON — MatchID Metrology beyond colors

Other partners: CAPACITÉS De la recherche à l'innovation — CARBON AXIS — CETIM

Depestele — EikoSim — ELSEVIER — FAIRMAT

metravib material testing — NOVITOM — Quantiflex simulations — Surface Measurement Systems World Leader in Sorption Science

Hosting Organizations

Conference chairs

Prof. Christophe BINETRUY
ECCM21 Conference Chair
Institute of Civil Engineering and Mechanics (GeM)
Centrale Nantes
Nantes Université

Prof. Frédéric JACQUEMIN
ECCM21 Conference Co-Chair
Institute of Civil Engineering and Mechanics (GeM)
Nantes Université

International Scientific Committee

Malin Akermo (Sweden)
Remko Akkerman (Netherlands)
Andrey Aniskevich (Latvia)
Leif Asp (Sweden)
Emmanuel Baranger (France)
Janice Barton (UK)
Johnny Beaugrand (France)
Andrea Bernasconi (Italy)
Christophe Binetruy (France)
Thomas Bohlke (Germany)
Alain Bourmaud (France)
Nicolas Boyard (France)
Joël Breard (France)
Richard Butler (UK)
Baris Caglar (Netherlands)
Pedro Camanho (Portugal)
Pierpaolo Carlone (Italy)
Paolo Andrea Carraro (Italy)
Valter Carvelli (Italy)
Nuno Correia (Portugal)
Gergely Czél (Hungary)
Clemens Dransfeld (Netherlands)
Sylvain Drapier (France)
Klaus DRECHSLER (Germany)
Andreas ECHTERMEYER (Norway)
Paolo Ermanni (Switzerland)
Martin Fagerström (Sweden)
Ewald Fauster (Austria)
Julien Ferec (France)
Antonio Ferreira (Portugal)
Bodo Fiedler (Germany)
Stefanos Giannis (UK)
Nathalie Godin (France)
Carlos Gonzalez (Spain)
Sotirios Grammatikos (Norway)
Christoph Greb (Germany)
Emile Greenhalgh (UK)
Gianmarco Griffini (Italy)
Stephen Hallett (UK)
Nahiene Hamila (France)
Roland Hinterhoelzl (Austria)
Martin Hirsekorn (France)
Darko Ivančević (Hungary)
Frédéric Jacquemin (France)
Mikko Kanerva (Finland)
Luise Karger (Germany)
Vassilis Kostopoulos (Greece)
Theodosia Kourkoutsaki (Germany)
Thomas Kruse (Germany)
Ugo Lafont (France)
Jacques Lamon (France)
Frédéric Laurin (France)
Antoine Le Duigou (France)
Stepan Lomov (Belgium)
Theodoros Loutas (Greece)
Staffan Lundstrom (Sweden)
António Marques (Portugal)
David May (Germany)
Véronique Michaud (Switzerland)
Jörg Mussig (Germany)
Thomas Neumeyer (Germany)
Philippe Olivier (France)
Alkiviadis Paipetis (Greece)
Federico Paris (Spain)
Chung Hae Park (France)
John-Alan Pascoe (Netherlands)
Alessandro Pegoretti (Italy)
Ton Peijs (UK)
Rob Pierce (Denmark)
Soraia Pimenta (UK)
Silvestre Pinho (UK)
Gerald Pinter (Austria)
Connie Qian (UK)
Marino Quaresimin (Italy)
Andrew Rhead (UK)
Paul Robinson (UK)
Essi Sarlin (Finland)
Yentl Swolfs (Belgium)
Sofia Teixeira du Freitas (Netherlands)
Julie Teuwen (Netherlands)
Ole Thomsen (UK)
Stavros Tsantzalis (Greece)
Konstantinos Tserpes (Greece)
Albert Turon (Spain)
Julien van Campen (Netherlands)
Wim Van Paepegem (Belgium)
Anastasios Vassilopoulos (Switzerland)
Ignaas Verpoest (Belgium)
Michael Wisnom (UK)
Dimitrios Zarouchas (Netherlands)
Daiva Zeleniakiene (Lithuania)
Dan Zenkert (Sweden)

Local Organizing Committee

Suresh Advani
Romain Agogué
Sylvain Chataigner
Sébastien Comas-Cardona
Sofiane Guessasma
Suzanne Laïk
Philippe Le Bot
Mael Peron
Luisa Silva
Vincent Sobodka
Alexandre Ripoche
Elena Syerko

Table of Contents

FINITE ELEMENT INVESTIGATION OF "CRADLE TESTS" FOR THE MECHANICAL CHARACTERIZATION OF PULTRUDED RODS UNDER COMPRESSION

Nicolas S.T. Darras[1], Iheoma Nwuzor[1], Ian R. Lee[1], Charlie Sharp[1], Curtis Wong[1], Gustavo Quino[2], Dimitrios Bikos[2], Bohao Zhang[1], Laura R. Pickard[1], Giuliano Allegri[1], Michael R. Wisnom[1] and Richard S. Trask[1]

[1]Bristol Composites Institute, School of Civil, Aerospace & Design Engineering, Queen's Building, University of Bristol, University Walk, Bristol, BS8 1TR, UK
Email: : nicolas.darras@bristol.ac.uk, Iheoma.nwuzor@bristol.ac.uk, ian.lee@bristol.ac.uk, gg20038@bristol.ac.uk, pz21288@bristol.ac.uk, Bohao.zhang@bristol.ac.uk, laura.pickard@bristol.ac.uk, Giuliano.Allegri@bristol.ac.uk, M.Wisnom@bristol.ac.uk, R.S.Trask@bristol.ac.uk
Web Page: https://bristol.ac.uk/composites

[2]Imperial College of London, South Kensington Campus, London, SW7 2AZ, UK
Email: d.bikos17@imperial.ac.uk, g.quino-quispe@imperial.ac.uk
Web Page: https://www.imperial.ac.uk/composites-centre

Keywords: Compression, pultruded rods, hybridisation, Mechanical testing

ABSTRACT
The development of hierarchical composites using pultruded rods as a primary building block is ongoing. These new composites, thanks to the nature of their constituent, offer more freedom of design as three-dimensional structures compared to the two-dimensional layer-by-layer composites. Getting a good understanding, and therefore characterisation of these building blocks becomes crucial before using them in hierarchical structures. However, it is expensive to perform many tests by following a trial-and-error approach. Modelling those tests therefore becomes useful as it allows the users to get a first estimation of the possible output of an experiment. These models are even more crucial when they aim to represent the complex behaviour of a system, as is the case with compression of Fibre Reinforced Polymers (FRPs): the shear instability, the buckling, twisting and rotations resulting from compression loads are not trivial to predict, neither are the limitations of the test method used. A model of a modified four-point bend test is presented, with its limits as well as its potential for improvement.

1. INTRODUCTION
Next Generation Fibre-Reinforced Composites (NextCOMP) [1] is a programme aiming to improve the compressive performance of composites. To do so, the development of hybridised, inspired by nature and hierarchical structures is investigated. Several routes are investigated to manufacture hierarchical composites. Thick plies and struts use highly aligned unidirectional pultruded rods [2]. These rods, when cured, can be used as the first base component to build composite parts, such as structural members (struts) by Resin Transfer Moulding [3], as depicted in Figure 1. Overbraiding rods can be done with a braider before using them to manufacture struts [4]. In addition of giving a wider design space for the composite structure, overbraiding rods is expected to improve their mechanical performance in compression, as shown by Wisnom [5] in his study of carbon fibre rods overwinded by Kevlar™. However, it is important to characterize the rods before using them in larger structures. A modified four-point bending test has been used for the characterization of regular pultruded rods [6]. Pickard *et al.* [4] show that using the modified four-point bend test method for cured overbraided rods leads to a failure

CONTENTS

of the beam before reaching the failure of the rod. Therefore, an update of this methodology is required to characterise the overbraided rods.

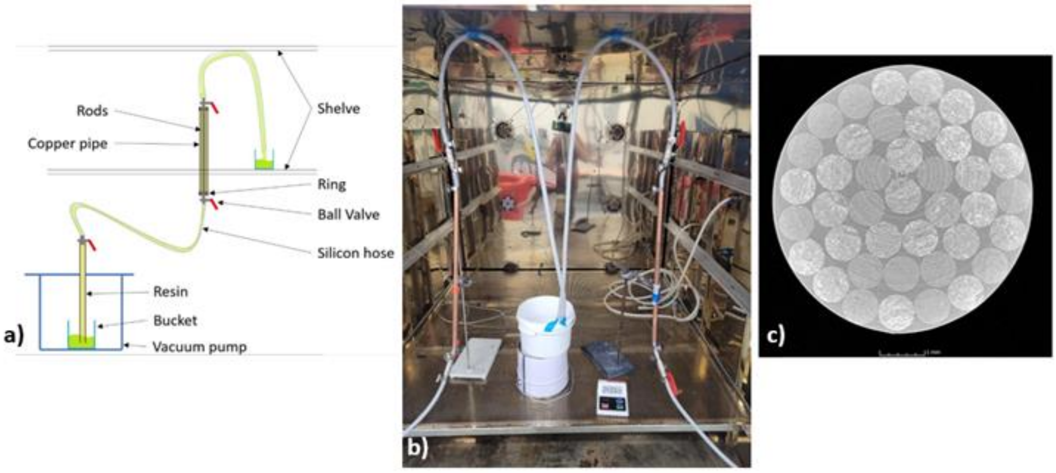

Figure 1. (a) Diagram of the Resin Transfer Moulding (RTM) process used to make struts, and (b) picture of the final setup for RTM at the National Composite Centre, and (c) CT-scan of the cross-section of one strut made with 40 CFRP rods, scan made with a Nikon XT H320, reproduced from [3].

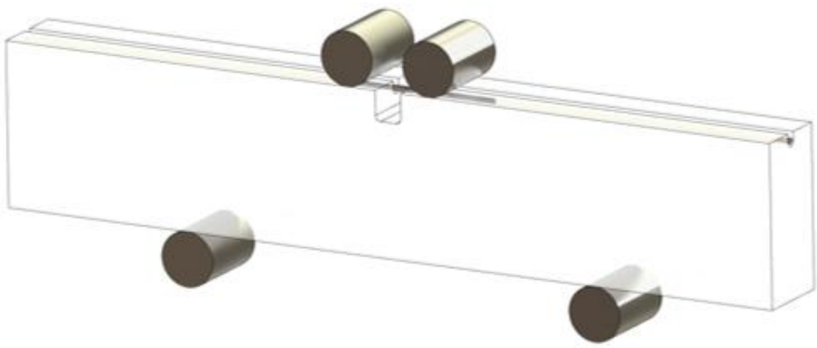

Figure 2. Schematic representing a composite rod embedded in a PMMA beam for a four-point bend test, reproduced from [6].

2. METHODS and MATERIALS

Regular carbon fibre reinforced polymer (CFRP) rods, supplied by Easycomposites, with a circular cross-section and a diameter of 0.8 mm [7] are bonded with an ethyl 2-cyanoacrylate adhesive [8] to a beam machined from poly(methyl methacrylate) (PMMA)[9], as per Lee *et al*. [10]. The method described by Pickard *et al*. [4] has been followed for the manufacture of overbraided rods, with the same equipment. The overbraided rods are then pulled through a bath of resin RS-M135 mixed with hardener RS-MH137 [11] with a modified pultrusion rig to wet and cure the overbraid. The pultrusion itself only brought the resin to a jelly phase enough to maintain the cross-section of the rod. However, a post-cure process at 50 °C for 10 hours must be followed to fully cure the resin. The cured overbraided rods are then bonded in the beam as per Lee *et al*. [10]. The methodology used by Quino *et al*. [6] and Lee *et al*.

CONTENTS

[10] is followed, using a Roell-Amsler universal test unit. The top loading noses, with a surface radius of 5mm, are spaced by 20 mm, and the bottom loading noses are 80 mm distant. Ten samples of 0.8 mm carbon fibre rods have been tested following this method. Five samples with cured overbraided carbon fibre are also tested with this test method. Furthermore, a finite element model of the modified four-point bend test has been made using Abaqus 2018 (Dassault System Simulia Corp, USA). The behaviour of the materials used for the parts of the model was assumed linear elastic. Both the loading and support rollers were considered rigid parts. An investigation into the stiffness of the rods has been conducted: three rods were considered with stiffness values of 50 GPa, 80 GPa, and 140 GPa. For clarity reasons, the data presented in this study will be collected from the model with a rod at 80 GPa. The material properties assigned to the parts are summarised in Table 1.

Table 1. Finite element model input mechanical properties.

Specimen type	E, E_{11} (GPa)	E_2, E_3 (GPa)	υ ($\upsilon_{12}, \upsilon_{13}$)	υ_{23}	G_{12}, G_{13} (GPa)	G_{23} (GPa)
PMMA	3.2	-	0.33	-	-	-
CFRP rod	80	10	0.32	0.45	5	3.4
IM7/8552 skin	164	11.4	0.32	0.436	5.17	3.98
Loading / support Roller	Rigid	-	-	-	-	-

3. EXPERIMENTAL RESULTS

The tests performed on the regular rods were successful, achieving a strain at failure of 1.42 (± 0.2) % at an applied load of 5 (± 1) kN. The tests performed on the cured overbraided rods were not successful. The load applied to the beam reached a point where the beam failed before the rod. The video taken of the experiments showed that the beam failed in tension, with a crack initiated from the tension side of the beam and propagated to the middle of the gauge section. The rod failed after the beam, so no data was usable from these experiments. Since the test method used did not produce any data for the overbraided rods, a modification of this method is required for the characterisation of the rod specimen.

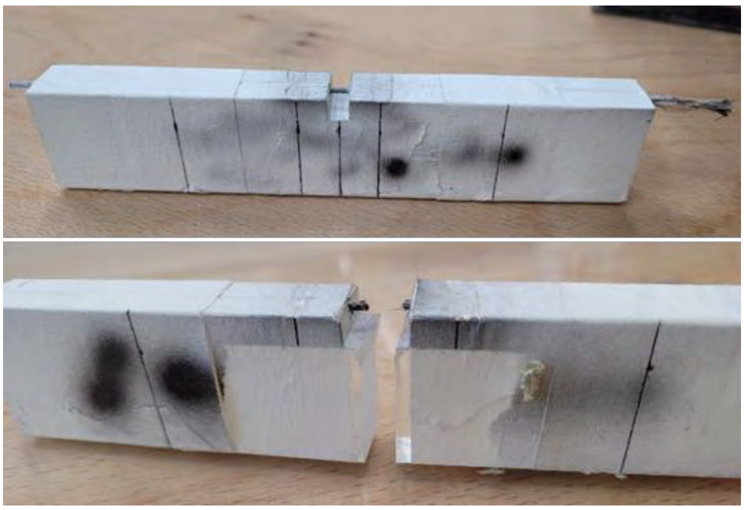

Figure 3. (Top) Photographs of the cradle beam with an overbraided rod, and (bottom) a broken cradle after test.

4. FINITE ELEMENT MODEL

The beam and the rod have been meshed with linear brick solid elements C3D8R. The size of the elements used was approximately 0.5 mm. For this model, the adhesive has been modelled as a tie interaction between the rod and the beam, considered perfect with no risk of debonding. A surface-to-surface contact has been defined between the noses and the beam, with a hard contact normal behaviour and penalty tangential behaviour with a friction coefficient of 0.15. The support noses are encastre and the top noses are loaded with a displacement of 1 mm as per Figure 4. This model has been used to estimate the bending test outputs for the single rods. An axial strain of 1.413% has been reached on the rod, in the middle of the gauge section, for a load of 5.8 kN. The load is 16% higher of what has been observed experimentally with this setup. However, it falls within the stated error as per section 3. A refinement of the rod's stiffness could also lead to more accurate correlation with the experimental work. Since the beam failed in tension, as shown in the experimental section, the focus has been put on investigating this failure. A comparison of the finite elements model with beam theory on the flexural tension stress seen by the beam has been done. Figure 5 is a schematic of the four-point bend test performed on the beam, the features such as the tunnel for the rod and the gauge section have not been represented for simplicity, leading to a slight underestimation of the stress seen on the tension side. Figure 5 is a simplification of the cradle used for the bending test of the rod. A load F is applied on the top loading noses, both spaced by a distance w (20 mm). The beam rests on the bottom loading noses spaced by a distance L (80 mm). Its dimensions are h (30 mm) and b (15 mm) respectively its height and width. The point A is in the middle of the beam, on its tension side during the test.

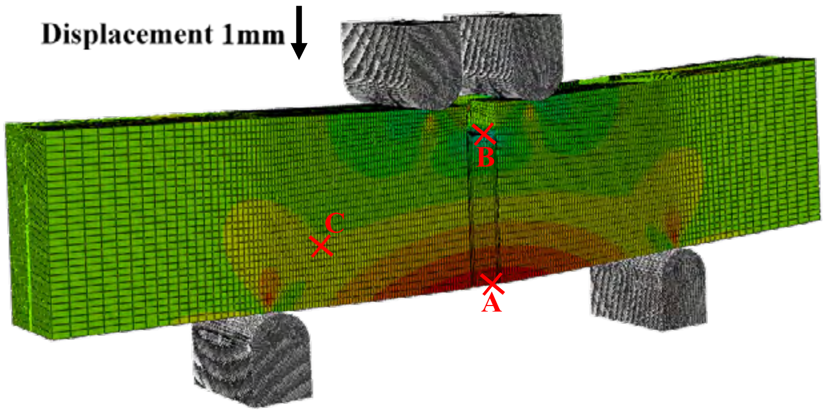

Figure 4. Finite element model of the four-point bend test performed on the regular rod, picture taken from Abaqus 2018. Points A, B and C are used for the collection of data.

Eq. (1) is the flexural moment seen at point A:

$$M_A = \frac{F}{4} * (L - w) \tag{1}$$

Eq. (2) represents the second moment of area of the cross-section of the beam:

$$I = \frac{b * h^3}{12} \tag{2}$$

Eq. (3) is the flexural tension stress seen at point A on the beam:

$$\sigma_A = \frac{M_A * c}{I} \tag{3}$$

By replacing Eq. (1) and Eq. (2) in Eq. (3), we get a direct expression of the stress at point A, σ_A:

$$\sigma_A = \frac{3}{2} * \frac{F * (L - w)}{b * h^2} \tag{4}$$

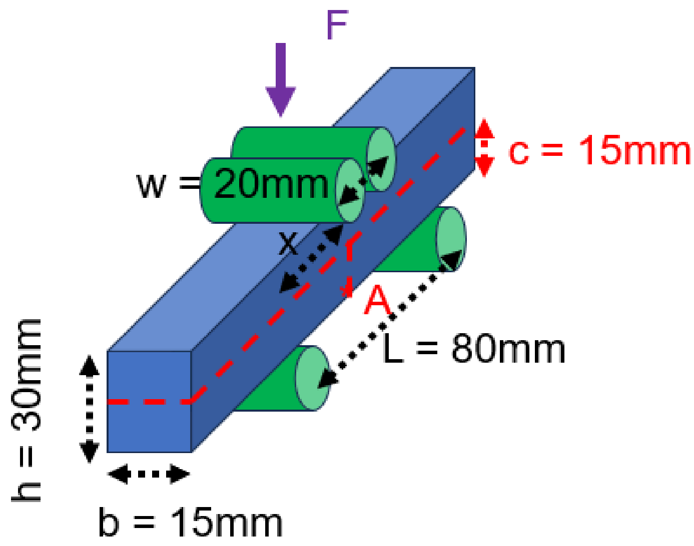

Figure 5. Schematic of the four-point bend test to perform a stress estimation at point A with the beam theory.

A numerical application of Eq. (4) with different load F and a comparison with the data obtained by the finite element model have been made. The results are shown in Table 2. The finite element model gives similar stress to the expected beam theory results, thus facilitating its application in investigating the modified four-point bend test method. As outlined in section 3, during trials with overbraided rods, the beam failure occurred prior to rod failure. Considering this, a substitution of the beam material with a stiffer alternative has been contemplated. However, opting for a stiffer alternative to carry a higher static load, such as typical aluminium alloy or glass fibre reinforced PEEK [12], would incur higher production costs. Nevertheless, such an alternative should ideally be reusable to facilitate testing of multiple rods. Consequently, the mechanical properties of the beam in the finite element model have been adjusted to reflect the stiffer alternative, and the resultant stress experienced by the beam at the rod failure strain has been documented. The findings of this investigation are presented in Table 3.

The flexural tension stress experienced by the beam at the rod's failure point escalates with the material's stiffness. This stress level is juxtaposed with the material's tension yield stress. It is evident that simply switching the beam material to aluminium would not suffice, as the yielding point would be surpassed with a standard rod. Consequently, the beam would not retain its reusability for testing other rods.
Another option investigated is to reinforce the beam with an IM7/8552 skin underneath. This modification would increase the flexural stiffness of the cradle used, thus reducing the stress on the PMMA beam. Furthermore, as the skin is very stiff compared to the beam (PMMA), it should bear most of the load, accentuating the positive impact on the beam. The skin covers the entire surface of the beam and is modelled as a unidirectional composite layup of eight plies (0.125 mm per ply) with the mechanical properties detailed in Table 1. The adhesive interaction between the beam and the skin has been modelled with a Tie constraint. Additionally, the surface-to-surface interaction between the skin and the support noses mirrors the interaction tilized for the beam and the loading noses.

Table 2. Stress at Point A obtained for the calculation and the FE model for different loads applied.

Load applied (N)	σ_A calculation (Mpa)	σ_A FE model (Mpa)
1500	10.0	10.3
5000	33.3	33.5
8000	53.3	53.4

Table 3. Investigation of the tension stress in the beam during bending with three different materials used for the beam.

Beam material	Young modulus (GPa)	Strain rod (%)	Flexural tension stress beam (MPa)	Tension stress to yield beam (MPa)
PMMA	3.2	1.42	38.6	75
Glass fibre PEEK	7.0	1.42	67.8	116
Aluminium alloy	70.0	1.42	431	400

Table 4. Comparison of the tension, compression and shear stress of the beam with and without a CFRP reinforcement skin at the failure points of the rod.

Parameter	PMMA beam	PMMA beam (with IM7/8552 skin)
Strain rod (%)	1.42	1.42
Flexural tension stress beam (MPa), Point A	38.6	5.8
Flexural tension stress skin IM7/8552 (MPa)	N/A	482.8
Compression stress beam (MPa), Point B	43.3	51.1
Shear stress beam (MPa), Point C	10.1	16.2
Von Mises stress beam (MPa), Point C	17.5	28.9
Load applied (kN)	5.8	10.8

The data presented in Table 4 are derived from identical nodes situated along the tension side of the beam, specifically at its midpoint represented by point A in Figure 4 for the flexural tension stress. The compressive stress has been collected from the midpoint of the notch section, represented by point B in Figure 4. Finally, the shear and Von Mises stresses have been collected between the upper and lower noses, represented by point C in Figure 4, along the load pathway. In the existing design, the tension stress experienced by the beam at the rod's failure point measures approximately 38 MPa. Following the addition of a skin beneath the beam, a measurement was taken at the same location, revealing a notable reduction in stress experienced by the PMMA beam to 5.8 MPa. Conversely, the stress endured by the skin is higher, at 482.8 MPa, correlating to a strain of 0.295% for this material. A higher load is required to reach the failure point of the rod due to the presence of the skin. This modification leads to a higher shear and compressive stress on the PMMA beam.

5. DISCUSSION and FUTURE WORK

The finite element model devised to simulate the adapted four-point bend test method employed in characterising pultruded rods has been made. At a load of 5.8 kN, the strain at the rod's midpoint registers at 1.4%, not far from the experimental observations for Easycomposite carbon fibre pultruded rods. Furthermore, the comparison of flexural tension stress experienced by the beam between the finite element model and theoretical beam calculations exhibits consistency. An experimental determination of the rod's stiffness must be achieved to implement in our model.

The possibility of substituting the beam material with a more rigid alternative for conducting the test with a reusable beam has been investigated. Nonetheless, analysis conducted using the finite element model indicates that employing aluminium would lead to reaching the yielding point with a standard rod. Additionally, utilising PEEK material, although feasible, would be cost-prohibitive and non-reusable due to the irreversible nature of the adhesive bonding process in the slot. Thus, altering the material is deemed unsuitable for modifying the methodology, necessitating instead a revision of the design geometry.

The addition of an IM7/8552 skin beneath the beam markedly reduced the stress experienced by the PMMA beam. Notably, due to its higher stiffness compared to PMMA, the skin predominantly bears the tension load. The observed stress reduction is considerable, indicating a promising avenue for characterizing overbraided rods. The strain endured by the skin upon failure of a standard rod is approximately 0.29%, allowing a margin before failure, as shown by Lovejoy *et al*. [13] who reported a failure strain in tension for IM7/8552 between 1.54% and 1.64% for a unidirectional composite. Furthermore, this modification induced higher compressive and shear stress in the PMMA beam. The compression stress observed with this new configuration is 51.1 MPa, which is lower than the tensile strength of the material as indicated in Table 3, and consequently lower than its compressive strength as well [14]. The maximum shear strength of the material, estimated from the maximum tensile strength of PMMA and applying the Von Mises criterion in pure shear, is 43.3 MPa. At the failure point of the rod, the beam also experiences a maximum Von Mises stress of 28.9 MPa at point C, mainly due to shear and some compression. This stress is lower than the yield stress of 75 MPa, meaning there is a margin before failure. The finite element model developed for this project shall be updated with overbraided rods. An estimation of their mechanical properties will be useful in developing the new test method. This model of an overbraided rod can then be used in developing a model of the hierarchical strut (Figure 1).

6. CONCLUSIONS

Developing a finite element model for a test method enables the manipulation of various parameters and exploration of outcomes without substantial expenditure of time and resources in laboratory settings. Utilising this approach, several studies have been conducted on the modification of a four-point bend test. The substitution of the material used for the beam with a stiffer alternative to prevent failure in tension creates a new challenge to overcome within the test methodology. The addition of a CFRP skin to the beam has also been investigated, showing a significant reduction in the stress experienced by the PMMA material as the load is primarily borne by the skin. This modification offers the advantage of being a simple additional step during the manufacture of the specimen and allows for a meaningful comparison with the rods already tested using the previous method.

Acknowledgments

The authors kindly acknowledge the funding for this research provided by UK Engineering and Physical Sciences Research Council (EPSRC) programme Grant EP/T011653/1, Next Generation Fibre-Reinforced Composites: a Full Scale Redesign for Compression (NextCOMP) a collaboration between Imperial College London and University of Bristol. For the purpose of open access, the authors has

applied a creative commons attribution (CC BY-NC 4.0) license to any author accepted manuscript version arising.

References

[1] NextCOMP, "Next Generation Fibre-Reinforced Composites: A Full Scale Redesign for Compression," www.nextcomp.ac.uk. Accessed Apr. 17, 2024.
[2] L. R. Pickard, G. Allegri, and M. R. Wisnom Manufacturing Advances for Pultruded Rod Based Structural Members and Thick Ply Systems. In *20th European Conference on Composite Materials*, *ECCM20*, Vol B, pages 170-177, 2022. doi: 10.5075/epfl-298799_978-2- 9701614-0-0.
[3] L.R.Pickard, J.Crinson, N.Darras, G.Allegri and Michael R.Wisnom. Evaluation of manufacturing methods for pultruded rod based hierarchical composite structural members with minimal porosity. *Rubber and Composites: Macromolecular Engineering*, Volume 53, Pages 25-35, 2024, doi: 10.1177/14658011231212627.
[4] L. R. Pickard, G. Allegri, and M. R. Wisnom. Overbraiding of Pultruded Rods for Hierarchical Composites. In *23rd International Conference on Composite Materials, ICCM23*, 2023, https://iccm-central.org.
[5] M. R. Wisnom. Suppression of splitting and impact sensitivity of unidirectional carbon-fibre composite rods using tensioned overwind. *Composites Part A: Applied Science and Manufacturing*, Volume 30, no. 5, pages 661–665, 1999, doi: 10.1016/S1359-835X(98)00174-2.
[6] G.Quino, P.Robinson, R.S.Trask. Design of a bending experiment for mechanical characterization of pultruded rods under compression. In *20th European Conference on Composite Materials, ECCM20.* Volume C, pages 167-172, 2022. doi: 10.5075/epfl-298799_978-2- 9701614-0-0
[7] 0.8 mm Carbon Fibre Rod – Easycomposites. Available: . Accessed Apr. 17, 2024.
[8] "Safety Data Sheet - Gorilla Super Glue". Available: www.gorillatough.com. Accessed: Apr. 17, 2024.
[9] I.R. Lee, M.L. Longana, L.R. Pickard, I. Hamerton and G. Allegri. Characterisation of highly-aligned, discontinuous fibre composites for compressive performance. In *23rd International Conference on Composite Materials, ICCM23*, 2023, https://iccm-central.org.
[10] "Perspex® Design Guide", Perspex. Available: www.perspex.co.uk. Accessed : May 15, 2024
[11] "RS-M135 – Epoxy Resin System Product Data", PRF Composite Materials. Available: https://www.prfcomposites.com. Accessed: Apr. 17, 2024.
[12] Glass fibre reinforced PEEK – Theplasticshop. Available: https://www.theplasticshop.co.uk/ . Accessed Apr. 28, 2024
[13] A.E. Lovejoy, S.T. Scotti, S.G. Miller, P. Heimann and S.S. Miller. Characterization of IM7/8552 Thin-ply and Hybrid Thin-ply Composites. *NASA NF1676L-30257*, 2020. Available: NASA STI Repository (NTRS)
[14] B. Zheng, S. Zhang, G. Shu, Z. Sun, Y. Wang and J. Xie. Experimental investigation and modeling of the mechanical properties of construction PMMA at different temperatures. *Structures*, Volume 57, 2023, doi: https://doi.org/10.1016/j.istruc.2023.105091

ECCM21

02-05 July 2024 | **Nantes - France**

Volume 8

Special Sessions

ISBN: 978-2-912985-01-9
DOI: 10.60691/yj56-np80